International Journal of Biochemistry and Cell Biology 106 (2019) 57–67

Contents lists available at ScienceDirect

International Journal of Biochemistry and Cell Biology

journal homepage: www.elsevier.com/locate/biocel

TNFα stimulates NO release in EA.hy926 cells by activating the CaMKKβ-AMPK-eNOS pathway

Dorota Dymkowska[a,*], Beata Drabarek[a], Anna Michalik[a], Natalia Nowak[b], Krzysztof Zabłocki[a,*]

[a] Laboratory of Cellular Metabolism, Nencki Institute of Experimental Biology of the Polish Academy of Sciences, 3 Pasteura Str., 02-093 Warsaw, Poland
[b] Laboratory of Imaging Tissue Structure and Function, Neurobiology Center, Nencki Institute of Experimental Biology of the Polish Academy of Sciences, Poland

ARTICLE INFO

Keywords:
AMP-activated protein kinase
Endothelial cells
Endothelial nitric oxide synthase
Proinflammatory response
Tumour necrosis factor α

ABSTRACT

Previously we showed that a mild stimulation of EA.hy926 cells with tumour necrosis factor alpha (TNFα) activated mitochondrial biogenesis, probably as a mechanism preventing cell death. This was accompanied by an increased phosphorylation of eNOS and elevation of NO release. The aim of the present study was to explain the biochemical basis of this effect. Our results indicate that eNOS is the only enzyme catalysing NO generation in EA.hy926 cells, and TNFα stimulates its activity by activating AMP-activated protein kinase (AMPK). Inhibition of AMPK with Compound C prevents the TNFα-induced activatory phosphorylation of endothelial nitric oxide synthase (eNOS) at Ser1177 and reduces the NO release. AMPK is activated by phosphorylation catalysed by liver kinase B1 (LKB1) and calcium/calmodulin-dependent protein kinase kinase beta (CaMKKβ), which are phosphorylated and thereby activated in the presence of TNFα. Moreover, CaMKKβ catalyses an activatory phosphorylation of sirtuin 1, which could deacetylate and activate eNOS both directly and indirectly by an elevating the LKB1 activity. TNFα hardly increases the nuclear fraction of sirtuin 1, thus its major activity is probably attributed to the cytosolic pool. This is in line with the elevated activity of eNOS. We conclude that the increased AMPK–dependent phosphorylation of eNOS at least partially explains the stimulation of NO generation by TNFα in EA.hy926 cells.

1. Introduction

Nitric oxide is a pleiotropic signalling molecule which regulates a wide spectrum of cellular processes. In particular it is a key regulator in the cardiovascular system, where it modulates the vascular tone and consequently controls the blood flow and pressure. NO also influences the immune response and oxidative stress-sensitive processes, prevents platelet aggregation thereby preventing excessive blood clotting, and activates anti-inflammatory cell responses (Hinder et al., 1999; Khaddaj Mallat et al., 2017). In vascular smooth muscle cells NO activates guanylate cyclase to stimulate their relaxation and therefore vasodilatation (Childers and Garcin, 2018). In addition, NO reversibly inhibits oxidative phosphorylation by competing with oxygen for cytochrome *c* oxidase (Poderoso et al., 1996). It also reacts with molecular oxygen and reactive oxygen species generating diverse reactive oxidation products (Subelzu et al., 2015). Thus, an abnormal NO generation or reduction of its availability may have severe deleterious effects on the blood circulatory system (Godo et al., 2016) and other key bodily functions.

NO is produced from L-arginine in a reaction catalysed by nitric oxide synthase (NOS). In mammalian cells three isoenzymes of NOS encoded by different genes have been identified: neuronal (nNOS), inducible (iNOS) and endothelial (eNOS). eNOS is expressed constitutively in many types of cells, including endothelial ones and is activated in response to diverse stimuli. The physiological function of the nitric oxide synthases is determined chiefly by their intracellular localization and posttranslational modifications. eNOS is a membrane bound protein mainly found in the caveolae of the plasma membrane and in the Golgi apparatus (Chen et al., 2013; Feron et al., 1996; Forstermann and Sessa, 2012).

The reaction catalysed by eNOS is the predominant source of NO in the vasculature. A number of precisely controlled mechanisms and signalling pathways related to the subcellular localization, post-translational modifications (phosphorylation and acetylation) and

Abbreviations: ACC, acetyl-CoA carboxylase; AMPK, AMP-activated protein kinase; $[Ca^{2+}]_c$, cytosolic Ca^{2+} concentration; CaMKII, calcium/calmodulin dependent kinase II; CaMKKβ, calcium/calmodulin-dependent protein kinase kinase beta; eNOS, endothelial nitric oxide synthase; LKB1, liver kinase B1; Sirt1, sirtuin 1; TNFα, tumour necrosis factor α

* Corresponding authors.
E-mail addresses: d.dymkowska@nencki.gov.pl (D. Dymkowska), k.zablocki@nencki.gov.pl (K. Zabłocki).

https://doi.org/10.1016/j.biocel.2018.11.010
Received 23 July 2018; Received in revised form 6 November 2018; Accepted 20 November 2018
Available online 22 November 2018
1357-2725/

interactions with regulatory proteins such as calmodulin and HSP90 regulate eNOS activity (Rafikov et al., 2011). The participation of calmodulin in eNOS activation indicates that an increase in $[Ca^{2+}]_c$ is an essential factor for eNOS activation but additional mechanisms are also possible. Moreover only dimeric eNOS is capable of producing NO while its monomeric form generates $O_2^{-\cdot}$ instead (Forstermann and Sessa, 2012). Phosphorylation of eNOS Ser1177 by any of a number of kinases: protein kinase B (Akt), cyclic AMP-dependent protein kinase (PKA), AMPK or Ca^{2+}/calmodulin-dependent protein kinase II (CaMKII) is one of the major means of its activation (Vanhoutte, 2018). On the other hand, phosphorylation of threonine 495 or acetylation of lysine 497 and 507 located in the calmodulin binding domain of eNOS prevents the interaction of eNOS and calmodulin thereby inhibiting the enzyme (Greif et al., 2004; Heiss and Dirsch, 2014; Watts and Motley, 2009). Therefore the important stimulatory modification of eNOS is carried out by sirtuin 1 (Sirt1), which catalyses eNOS deacetylation. This reaction is possible only if Sirt1 is present in the cytosol (Mattagajasingh et al., 2007).

TNFα is a pro-inflammatory cytokine which activates a broad spectrum of cellular processes. It is essential for the proper response of cells to infection, during haematopoiesis, immunological reactions or tumour regression. However, excessive concentrations of TNFα may be harmful (Aggarwal, 2003). The vascular endothelium is an important target for TNFα, where it induces expression of genes mainly associated with pro-inflammatory responses and cell proliferation. We have reported earlier that stimulation of EA.hy926 cells with TNFα induces pro-survival changes in the mitochondrial metabolism and architecture and activates mitochondrial biogenesis, which we interpreted as a rescue mechanism preventing cell death (Drabarek et al., 2012). The elevated levels of mitochondrial proteins and transcription factors were accompanied by an increased generation of NO. Although TNFα-induced production of NO has been reported by other authors as well (Kalogeris et al., 2014; Francis et al., 2001), its mechanism in endothelial cells has not been established. Here we continue the previous study by investigating the biochemical foundations of the TNFα–induced stimulation of NO synthesis. In particular we show that eNOS is the only isoform responsible and identify a multi-step mode of its activation.

2. Material and methods

2.1. Cells

Immortalized human umbilical vein endothelial cells, line EA.hy926, passage 1–12 (passage "0" - cells purchased from the ATCC) were grown in low glucose (1 mg/ml) Dulbecco's Modified Eagle Medium (DMEM) supplemented with 10% foetal bovine serum (Gibco Invitrogen), antibiotics (penicillin 100 units/ml plus streptomycin 100 μg/ml, Sigma) in a humidified atmosphere of 5% CO_2 /95% air at 37 °C. The growth medium was changed every two days. Confluent cells were treated with 5 or 10 ng/ml TNFα (as indicated) for 6 h.

2.2. NO determination

Secreted NO was determined with DAF-FM (4-amino-5-methylamino- 2′,7-difluorescein, non-esterified form; Molecular Probes, D-23841), which does not enter cells and only reacts with NO in the incubation solution. Cells grown on 6-well plates were prepared according to a previously published protocol (Dymkowska et al., 2017). After addition of 0.1 μM DAF-FM cells were incubated for 30 min and fluorescence was measured using a Shimadzu RF-5000 spectrofluorimeter. Cells treated with L-NAME (eNOS inhibitor) were used to distinguish eNOS activity from other potential sources of NO.

Table 1
TaqMan probes used for RT-qPCR analysis of *NOS* transcripts.

Gene	Catalog number	Product size	UniGene number
nNOS	Hs00167223_m1	61	Hs.647092
iNOS	Hs01075529_m1	67	Hs.709191
eNOS	Hs01574659_m1	107	Hs.654410
HRPT1	Hs99999909_m1	100	Hs.412707
YWHAZ	Hs00237047_m1	70	Hs.492407

2.3. mRNA isolation and RT-qPCR

RNeasy Mini Kit (Qiagen) was used for isolation of total RNA as described in the manufacturer's instruction. RNA concentration and purity was determined using a NanoDrop Microvolume Spectrophotometer (Eppendorf) by measuring optical densities at 260 and 280 nm. RNA purity was deemed satisfactory if the OD 260/280 nm ratio was 1.8–2.0. Samples were stored at −80 °C.

Reverse transcription was done with the use of First Strand cDNA Synthesis Kit (Thermo Scientific) according to the manufacturer's protocol. Negative controls (without enzyme) for each sample were prepared as described in the same protocol. cDNA concentration was determined as in the case of RNA. OD 260/280 ratio > 1.7 was accepted as a marker of sufficient purity. Samples were stored at −20 °C.

qPCR reaction was performed with the use of a 7500 Real-time PCR System (Applied Biosystem) in 20 μl of a reaction mixture consisting of 1.5 μl of cDNA (100 ng/ml), 10 μl of Universal PCR Master Mix (Roche Diagnostic Ltd.), 1 μl of TaqMan probe and RNA-se free water. Transcript of the hypoxanthine phosphoribosyl transferase gene (*HRPT1*) was used as reference (Żyżyńska- Granica and Koziak, 2012). All TaqMan probes used are listed in Table 1. Experimental data were analysed using the comparative method ($\Delta\Delta C_t$) and Life Technologies 7500 Software v 2.0.6.

2.4. Cell lysis and Western blot analysis

Cell lysates were prepared as previously (Drabarek et al., 2012). Proteins were separated by PAGE under denaturing conditions in the presence of 0.1% sodium dodecylsulfate. After transferring onto a PVDF membrane proteins of interest were detected with specific primary antibodies. Secondary antibodies were conjugated with horseradish peroxidase (HRP). All primary and secondary antibodies used are listed in Table S1. Chemiluminescent substrate (Luminata Classico, Millipore) was used for HRP detection. Optical density of bands corresponding to individual proteins was estimated using Fusion FX (Vilber Lourmat) and BIO-1D software and expressed in relation to β-actin used as a loading control.

2.5. Immunocytochemistry

For visualization of Sirt1, cells grown on coverslips were fixed with 4% paraformaldehyde, rinsed with PBS and permeabilized with 0.01% Triton X-100 in PBS containing 1% bovine serum albumin (BSA). After blocking with 5% BSA cells were incubated overnight with primary anti-Sirt1 or anti-pSirt1 antibody (Cell Signaling Technology) in 1% BSA dissolved in PBS, rinsed with PBS and incubated with secondary antibody conjugated with Alexa Fluor 555 (Cell Signaling Technology) in PBS containing 1% BSA. Finally, the cells were sealed in VECTASHIELD Mounting Medium (VECTOR Laboratories) containing DAPI to visualize nuclei. Fluorescence microscopy was carried out using a Zeiss Spinning Disc Microscope. For nuclear Sirt1 intensity analysis, maximum projection images were obtained from the Z-stacks in ImageJ software. Such images of the DAPI channel were subjected to background subtraction using the Rolling Ball method. The resulting images were analysed using custom pipelines in CellProfiler 3.0 software. The values for integrated or mean red fluorescence intensity for Sirt1 and

pSirt1 were compared.

2.6. Determination of intracellular calcium concentration

Cells grown on 24-well plates were incubated with 2 μM Fluo-4-AM (Molecular Probes) for 30 min in the culture medium, rinsed carefully and 0.5 ml medium was added to each well. The cells were incubated for additional 30 min to allow full de-esterification of the intracellular dye. The intensity of fluorescence was measured using laser scanning cytometer (iCYS, CompuCyte) equipped with the laser 488 nm and the filter for green fluorescence (530 ± 30 nm).

2.7. Cell fractionation for detection of activated PKCα

To assess activation of PKCα, which is connected with its translocation from the cytosol to the plasma membrane, EA.hy926 cells were fractionated (Kowalczyk et al., 2009). Cells grown on 10-cm culture dishes were rinsed with ice-cold PBS and homogenized in a Potter-Elvehjem homogenizer in 1 ml of ice-cold isotonic buffer (15 mM Tris/HCl, pH 7.6; 0.25 M sucrose; 1 mM DTT; 0.5 mM PMSF; protease and phosphatase inhibitors). Then a 50-μl sample of the homogenate was supplemented with 5 μl (10xconc.) ice-cold lysis buffer. The remaining homogenate was centrifuged (1000xg for 10 min) at 4 °C, supernatant collected and the pellet suspended in isotonic buffer, homogenized and centrifuged again as above. The two supernatants were pooled and centrifuged at 14000xg for 20 min at 4 °C. The final supernatant (S1 fraction) was collected and stored at −20 °C. The pellet was suspended in lysis buffer and stored as P2 fraction (membrane fraction). Proteins of interest were determined by Western blotting using the plasma membrane Ca^{2+}-ATPase 2 (PMCA2) as a marker of the plasma membrane (Affinity BioReagents).

2.8. Determination of adenine nucleotides

Cells grown on 10-cm culture dish was rinsed in ice-cold 0.3 M mannitol and then 1.8 ml of extraction mixture containing methanol, acetonitrile and water (2:2:1/v:v:v) was added. After extraction (5 min on ice) 1.5-ml portion of the extract was centrifuged at 12000xg for 5 min at 4 °C. Supernatant was stored at −80 °C. ATP, ADP and AMP were separated in KOH gradient and quantitated by HPLC using IonPac AS-11HC analytical column and IonPac AG11-HC guard column. Determination of adenine nucleotides content was performed in UV light at 260 nm and quantified from standard curve.

2.9. Protein determination

Protein was quantitated using a modified Lowry protein assay kit (ThermoScientific,).

2.10. Statistical analysis

Data shown are means ± S.D. for the number of separate experiments indicated in figure legends. Statistical significance of differences (p-values less than 0.05) were calculated using one-way analysis of variance (ANOVA). Duncan's Multiple Range Test was used for multigroup comparisons.

3. Results

3.1. eNOS and NO generation

Data shown in Fig. 1 confirm our previous findings that incubation of cells with TNFα elevates the release of NO to the incubation solution. To identify the isoform of NOS that is stimulated and therefore responsible for the increased NO synthesis we analysed the expression of NOS isoforms by Western blotting and RT-qPCR. Interestingly, neither

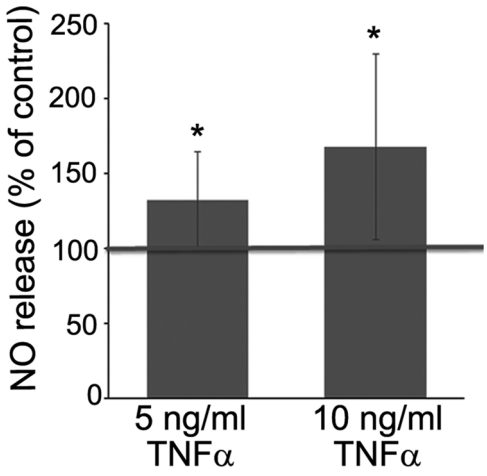

Fig. 1. Effect of TNFα on NO release.
EA.hy926 cells were incubated with TNFα at 5 or 10 ng / ml for 6 h. NO content in incubation medium was determined fluorimetrically with non-cell permeable DAF. NO release by control cells (not exposed to TNFα) is taken as 100% (horizontal grey lane). Mean ± SD from 10 independent experiments is shown; * $p < 0.001$ vs. control.

nNOS nor iNOS proteins could be detected in EA.hy926 cells with or without TNFα treatment, while eNOS was fairly abundant both before and after cell stimulation with TNFα (Fig. 2). To confirm the apparent absence of iNOS and nNOS we carried out RT-qPCR analysis for the respective mRNAs in control conditions and following TNFα action, finding no measurable expression of either gene in either condition (Fig. 2A and B). These results clearly indicated that the only enzyme responsible for the NO generation in EA.hy926 cells could be eNOS. Although the incubation of the cells with TNFα did not substantially elevate the total amount of eNOS protein, the fraction of this phosphorylated at the Ser1177 enzyme was significantly increased (Fig. 2C). This phosphorylation increases the enzymatic activity while an inhibitory phosphorylation at Thr495 (which prevents calmodulin binding) seems not to be affected upon TNFα treatment of cells (Fig. 3A). This is in line with the unchanged activity of PKCα which catalyses the latter phosphorylation (Fig. 3B) and indicates that TNFα does not elevate the eNOS activity by reducing its inhibitory phosphorylation. Since calmodulin binding is known to be required for eNOS activity, we reasoned that the eNOS activation by TNFα could be due to an increased Ca^{2+} concentration. Indeed incubation of cells with TNFα elevates $[Ca^{2+}]_c$ (Fig. 4A). It is noteworthy that also excitation of cells with histamine which leads to a massive elevation of $[Ca^{2+}]_c$, substantially increased eNOS phosphorylation at Ser1177 even in the absence of the TNFα (Fig. 4B).

3.2. AMPK phosphorylation

To define the mechanism of the activation of eNOS by TNFα we first turned to AMPK, known to carry out the Ser1177 phosphorylation of eNOS. In particular, TNFα did not affect the phosphorylation state of other kinases (Akt, CaMKII or PKA) which also were considered as enzymes catalysing activatory phosphorylation of eNOS (data not shown). It turned out that incubation of cells with TNFα activated AMPK itself, as evidenced both by its increased phosphorylation on Thr172 and increased phosphorylation of an important AMPK substrate, acetyl-CoA carboxylase (ACC). Its phosphorylation level is a convenient measure of AMPK activity (Fig. 5).

It is noteworthy that TNFα does not affect the content of adenine nucleotides in EA.hy926 cells (Table 2), therefore AMPK activation by an increased concentration of AMP and ADP seems unlikely. We further confirmed the major or, most likely, exclusive role of AMPK in the eNOS activation by using Compound C, a widely used AMPK inhibitor.

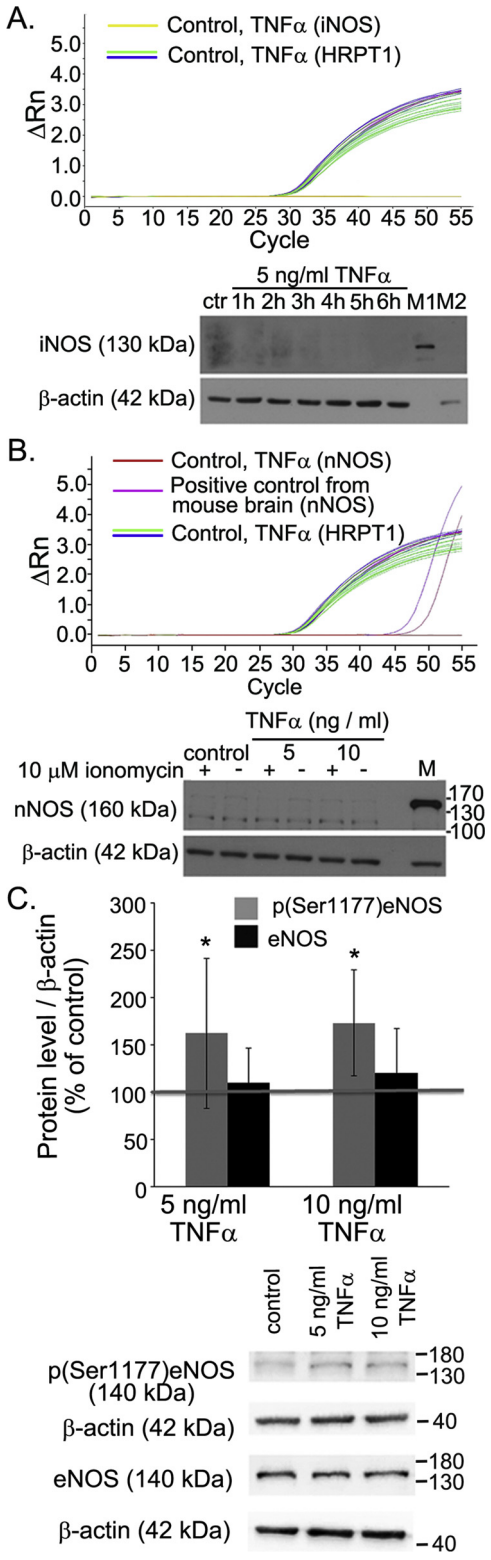

Fig. 2. Effect of TNFα on NOS expression and activity.
EA.hy926 cells were incubated with TNFα at 5 or 20 ng / ml for 6 h. mRNA was quantified by RT-qPCR with HRPT1 gene as reference. Protein levels were determined by Western blotting with β-actin as a loading control and optical density of bands was calculated densitometrically.
A. iNOS. Top: Representative amplification curves (out of 3 independent experiments): yellow line – iNOS (in control and TNFα treated cells); green and blue lines– reference HRPT1 gene (in control and TNFα treated cells). **Bottom**: Representative Western blot for iNOS (out of 3 independent experiments). Positive controls: M1 - commercially available lysate from murine macrophages treated with IFNγ / LPS (BD Transduction Laboratories, #611473); M2 – lysate from J774 cell line treated with 1000 ng / ml LPS for 6 h.
B. nNOS. Top: Representative amplification curves (out of 3 independent experiments): red line – nNOS (in control and TNFα treated cells); green and blue lines – reference HRPT1 gene (in control and TNFα treated cells); pink line – nNOS gene in the sample from mouse brain. **Bottom:** Representative Western blot for nNOS (out of 3 independent experiments). Positive controls M – lysate from mouse hippocampus.
C. eNOS. Relative **p**rotein levels of eNOS and p(Ser1177)eNOS normalized to β-actin content are shown. Representative values in control cells were taken as 100 (horizontal grey line). Mean ± SD from 15 independent experiments is shown; * $p < 0.001$ vs. control. Below representative Western blot.

In its presence virtually no induction of NO release upon TNFα action was observed (Fig. 6).

3.3. Phosphorylation of CaMKKβ, LKB1and Sirt1

The activatory phosphorylation of AMPK at Thr172 may be catalysed by either of the two upstream kinases, CaMKKβ and LKB1. The first one is a Ca^{2+}-dependent enzyme, so the TNFα-evoked increase of $[Ca^{2+}]_c$ suggested its involvement in the phosphorylation of AMPK. Indeed, CaMKKβ phosphorylation indicating its activation was increased in cells exposed to TNFα (Fig. 7A). Moreover, pre-incubation of cells with STO-609, an inhibitor of CaMKKβ, limited the TNFα-induced NO generation (Fig. 7B). However, this inhibitory effect was not complete, suggesting a contribution of LKB1 to the AMPK phosphorylation.

This conclusion was confirmed by showing that TNFα significantly increases the phosphorylation and thereby activity of LKB1 (Fig. 8). We were unable to verify directly its participation in AMPK phosphorylation since a specific inhibitor of LKB1 is not available. However, we found that TNFα increases the extent of phosphorylation of Sirt1 protein (Fig. 9A). Sirt1 may enhance AMPK activity directly or through LKB1 deacetylation (Lan et al., 2008), thus its phosphorylation (and activation) is in line with the other results shown hitherto. It is noteworthy that the phosphorylation of Sirt1 was not accompanied by its massive dislocation to the nuclei although some increase of nuclear pSirt1 content is observed. However the largest pool of phosphorylated Sirt1 was found in the cytoplasm (Fig. 9B), where it would be able to affect the cytoplasmic kinases LKB1 and AMPK and also eNOS itself. Notably, the TNFα–induced phosphorylation of Sirt1 required CaMKKβ activity as it was fully abrogated by the CaMKKβ inhibitor STO-609 (Fig. 10).

Altogether, the presented results indicate that the proinflammatory cytokine TNFα applied at a moderate concentration, much lower than that required to induce cell death, activates NO generation in EA.hy926 cells in an AMPK-dependent manner, which process is controlled by the upstream kinases LKB1 and CaMKKβ and likely also by Sirt1 deacetylase.

4. Discussion

Earlier we observed that a mild treatment of endothelial EA.hy926 cells with TNFα induced pro-inflammatory response accompanied by the pro-survival activation of NF-κB, changes in mitochondrial network organization and increase in the level of transcription factors required for mitochondrial biogenesis (Drabarek et al., 2012). We concluded that this response reflected a rescue mechanism supporting cell survival and metabolic integrity. Moreover, the earlier data as well as results presented here have clearly shown that the TNFα treatment substantially elevates the release of NO. An increased NO generation has been shown earlier by Szczygiel et al. (2012) for human dermal microvascular endothelial cells treated with TNFα (10 ng/ml) for 6 or 12 h and also by other authors (Fan et al., 2018; Kawanaka et al., 2002; Lamas et al.,

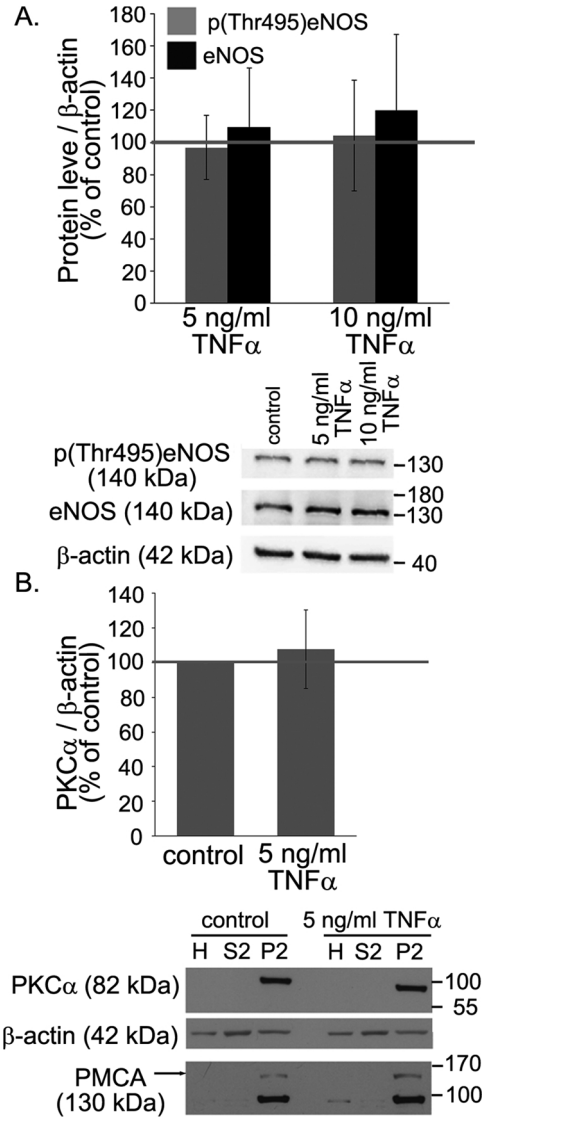

Fig. 3. Effect of TNFα on inhibitory phosphorylation of eNOS at Thr495 and PKCα activation.

EA.hy926 cells were incubated with TNFα at 5 or 10 ng / ml for 6 h.

Protein levels were determined by Western blotting with β-actin as reference. Optical density of bands was calculated densitometrically and normalized to β-actin.

A. p(Thr495)eNOS: Relative protein levels of eNOS and p(Thr495)eNOS content is shown. Representative values in control cells were taken as 100 (horizontal grey line). Mean ± SD from 15 independent experiments for eNOS (the data shown here are those shown on Fig. 2C) and 4 independent experiments for p(Thr495)eNOS is shown. **Bottom**: Representative Western blot.

B. PKCα: Relative protein levels of activated PKCα were determined by Western blotting in P2 fraction (related to plasma membrane) after cell fractionation. PMCA2 was used as a marker for plasma membrane. Representative values in control cells were taken as 100 (horizontal grey line). Mean ± SD from 4 independent experiments is shown. Below representative Western blot.

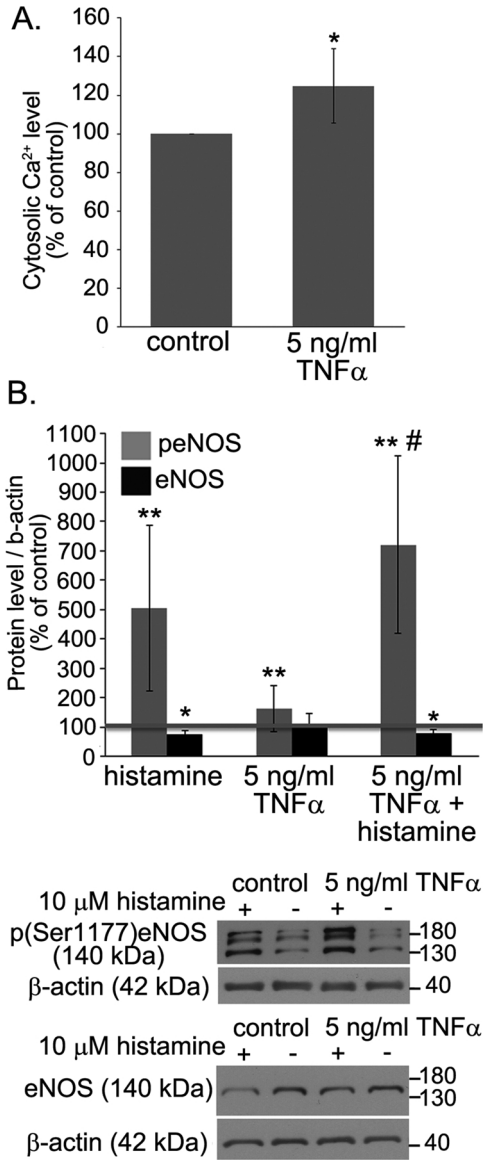

Fig. 4. Effect of TNFα on intracellular calcium concentration and Ca^{2+}-dependent eNOS phosphorylation at Ser1177.

EA.hy926 cells were incubated with TNFα at 5 ng / ml for 6 h.

A. Cytosolic calcium concentration was measured fluorimetrically with Fluo4 dye. Mean ± SD from 7 independent experiments is shown; * $p < 0.002$ vs. control.

B. Cells were stimulated with 10 μM histamine to induce massive increase of cytosolic Ca^{2+}. Relative **p**rotein level of eNOS and p(Ser1177)eNOS normalize to β-actin content are shown. Representative values in control cells were taken as 100 (horizontal grey line). Mean ± SD from 5 independent experiments is shown; * $p < 0.02$, ** $p < 0.001$ vs. control; # $p < 0.02$ vs. histamine alone. Below representative Western blot.

1991; Li et al., 2007). On the other hand, contradictory data indicating an inhibitory effect of TNFα on eNOS activity and endothelial NO generation have also been published (Choi et al., 2017; Liu et al., 2018). This discrepancy is difficult to solve and may be due to a number of factors. First of all, experimental conditions may dramatically influence the response of endothelial cells. Thus, a very high confluency of the cell monolayer is required to ensure a reproducible response to TNFα and its concentration and duration of treatment are critical. For these reasons a direct comparison of experimental data coming from various laboratories may be misleading. The results presented here were highly reproducible and convincingly show that EA.hy926 cells maintained at high confluency for 3 days and then exposed for 6 h to TNFα at a concentration of 5 or 10 ng/ml exhibit increased NO generation simultaneously with an elevated activatory phosphorylation of eNOS at the Ser1177 residue. The conditions used were sufficient to induce the pro-inflammatory response but too mild to affect viability of these cells (Drabarek et al., 2012).

NO synthesis is mainly catalysed by NOS family. iNOS is usually not detectable under resting conditions, but pro-inflammatory cytokines stimulate its expression in a number of cells (Aktan, 2004). However,

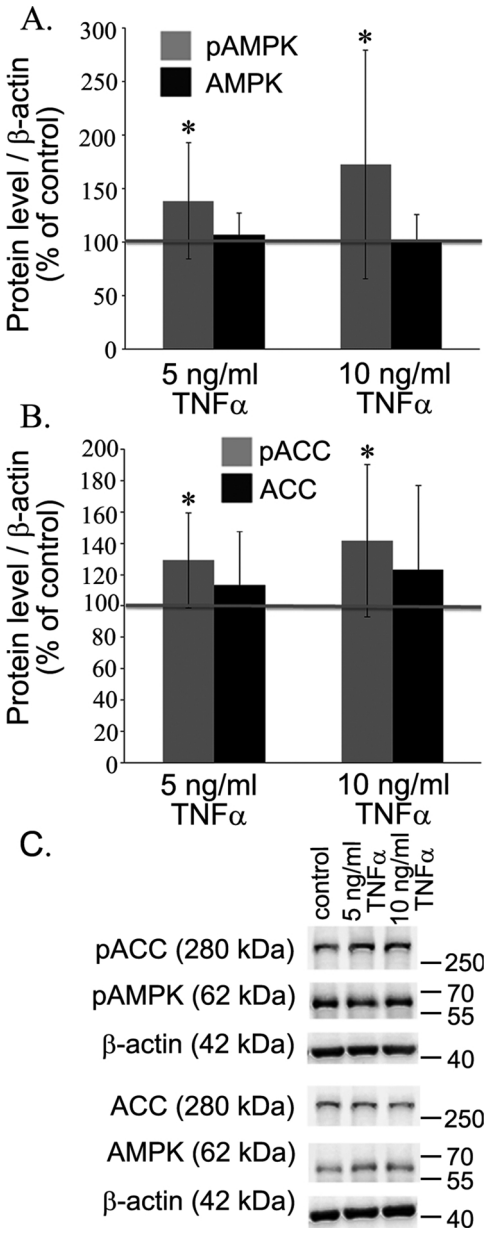

Fig. 5. Effect of TNFα on phosphorylation of AMPK at the Thr172 and phosphorylation of acetyl-CoA carboxylase (ACC).
EA.hy926 cells were incubated with TNFα at 5 or 10 ng / ml for 6 h.
Protein levels were determined by Western blotting with β-actin as reference. Optical density of bands was calculated densitometrically and normalized to β-actin.
A. Relative **p**rotein levels of pAMPK and AMPK are shown. Representative values in control cells were taken as 100 (horizontal grey line). Mean ± SD from 14 independent experiments is shown; * $p < 0.001$ vs. control.
B. Relative **p**rotein levels of pACC and ACC are shown. Representative values in control cells were taken as 100 (horizontal grey line). Mean ± SD from 15 independent experiments is shown; * $p < 0.05$ vs. control.
C. Representative Western blot for AMPK and ACC and their phosphorylated forms.

the absence of the iNOS transcript and protein in endothelial cells treated with TNFα, as found in the present study, should not to be surprising as iNOS has been reported to be induced only upon combined treatment of cells with a pro-inflammatory cytokine and IFN-γ (Kofler et al., 2005). Incidentally, the fact that eNOS turned out to be the only enzyme catalysing the NO generation in TNFα-treated cells greatly simplified the tracking of the signalling pathway involved in the stimulation of NO generation.

Table 2
Adenine nucleotide content in EA.hy926 cells following TNFα treatment.

	AMP	ADP	ATP
control	1	1	1
TNFα	1.12 ± 0.15	1.04 ± 0.2	0.97 ± 0.09

EA.hy926 cell were incubated with 5 ng / ml TNFα for 6 h. Data shown are mean ± SD from 4 experiments.

eNOS activity is regulated by diverse posttranslational modifications and is dependent on the $[Ca^{2+}]_c$ through the eNOS interaction with calmodulin. One of these modifications is phosphorylation, activatory on Ser1177 and inhibitory on Thr495. In endothelial cells the latter can only be catalysed by protein kinase C (PKC) (Fleming et al., 2001). Here it was shown that TNFα did not influence the Thr495 phosphorylation and did not alter PKCα activity, either, so it may be assumed that TNFα does not affect the eNOS activity by this mechanism. In contrast an increased eNOS phosphorylation at Thr495 in HUVECs has been shown to decrease its activity and reduce NO formation by reducing the binding of calmodulin (Greif et al., 2004; Li et al., 2004, 2016).

The substantially elevated phosphorylation of eNOS at Ser1177 following TNFα action found here is in agreement with previously published results (De Palma et al., 2006). Those authors found that the only activity of NOS in HUVECs exposed to TNFα (50 ng/ml) for 60 min could be attributed to eNOS, iNOS and nNOS being undetectable. Moreover, TNFα significantly increased the activity/phosphorylation of eNOS. In contrast, Neumann et al. (2004) reported that an exposition of bovine lung microvascular endothelial cells to TNFα (50 ng/ml) for 48 h caused a substantial inhibition of the eNOS gene expression and decreased the eNOS protein level. It seems plausible that a prolonged incubation (48 h instead of 6 h) with a high concentration of TNFα (50 ng/ml vs. 5 or 10 ng/ml) activates mechanisms other than those described here. One should note, e.g., that stimulation of HeLa cells with 100 ng/ml TNFα reduced cell viability by activation of apoptotic cell death (Bulotta et al., 2001). Those authors suggested that stimulation of eNOS and increased NO formation could protect cells against the cytokine-induced apoptosis.

eNOS protein phosphorylation is an important but not the only mechanism of its activation. Changing of $[Ca^{2+}]_c$ is another factor allowing eNOS activity to respond to extracellular stimuli (Devika and Jaffar, 2013). Even a slight TNFα-induced elevation of $[Ca^{2+}]_c$ could increase the eNOS activity by modulating its interaction with calmodulin or, in a more indirect manner, by stimulation of a specific protein kinases. We found that a short-term stimulation of EA.hy926 cells with histamine known to act by stimulating rapid increase in $[Ca^{2+}]_c$, significantly enhanced eNOS phosphorylation on Ser1177, confirming the latter possibility. Similar results have also been obtained by Li et al. (2003) on HUVECs and EA.hy926 cells in short-time experiments as well as after prolonged incubation with histamine that allowed them to observe an increased eNOS gene expression as well. As to the role of the elevated $[Ca^{2+}]_c$ in the TNFα-induced activation of eNOS we were unable to determine whether its action is exclusively direct, through calmodulin, or whether it also affects the Ser1177 phosphorylation via Ca^{2+}-dependent kinase such as CaMKII. We did not attempt using Ca^{2+} chelators (extracellular such as EGTA or intracellular such as BAPTA) since their action would inevitably lead to a profound modification of experimental conditions. We assume tentatively that the TNFα-induced increase in $[Ca^{2+}]_c$ affected eNOS both directly and - through stimulation of Ser1177 phosphorylation – indirectly.

Numerous protein kinases have been postulated to catalyse eNOS phosphorylation on Ser1177, including CaMKII (Murthy et al., 2017), Akt (Seifi et al., 2018), PKA (García-Morales et al., 2017) and AMPK (Cacicedo et al., 2011; Tanano et al., 2013). Here we found that upon

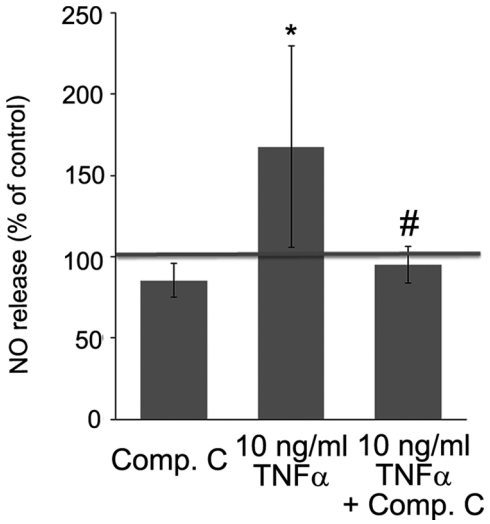

Fig. 6. Effect of Compound C on TNFα-induced NO release.
EA.hy926 cells were incubated with TNFα at 10 ng / ml for 6 h. 10 μM Compound C (Comp. C) was added for the last 20 min of incubation.
NO content in incubation medium was determined fluorimetrically with non-cell permeable DAF. NO release by control cells (not exposed to TNFα) is taken as 100% (horizontal grey lane). Mean ± SD from10 independent experiments for TNFα alone (the data shown here are those shown on Fig. 1) and 5 independent experiments for Compound C is shown; * $p < 0.001$ vs. control, # $p < 0.001$ vs. TNFα.

exposition of EA.hy926 cells to TNFα the total levels of Akt and CaMKII as well as the extent of their phosphorylation were not affected. Thus, their participation in the stimulation of NO release by TNFα seems unlikely. In contrast, the phosphorylation at Thr172 of the catalytic α subunit of AMPK and the Ser79 phosphorylation of ACC, an AMPK substrate, were significantly elevated indicating AMPK activation. Similar observations have been reported for bovine aortic endothelial cells stimulated with bradykinin (Mount et al., 2008) and EA.hy926 cells after LPS-evoked pro-inflammatory stimulation. It has been concluded that the activation of AMPK is a part of the cellular response to stress and could have a protective role against LPS-induced injury during sepsis (Escobar et al., 2015; Liu et al., 2016). Thus, the significantly increased phosphorylation of AMPK in cells incubated with TNFα could in a similar manner result from the pro-inflammatory activation of EA.hy926 cells manifested by an increased ICAM-1 protein level. As we showed earlier, it was accompanied by increased mitochondrial biogenesis interpreted as a mechanism protecting the cells against TNFα-induced cell death (Drabarek et al., 2012). It is accepted that the mitochondrial metabolism and biogenesis are, at least partially, controlled by AMPK (Inata et al., 2018).

A relationship between AMPK and eNOS in aortic endothelial cells has previously been shown in a mouse model of shear stress (Zhang et al., 2006). Similarly, an AMPK-mediated increase in NO generation due to elevated eNOS phosphorylation at Ser1177 has been shown in rat microvessels stimulated with AICAR (5-aminoimidazole-4-carboxamide-1-β-D-ribofuranoside), a direct AMPK activator (Bradley et al., 2010). Here, Compound C ({6-[4-(2-piperidin-1-yl-ethoxy)-phenyl]}-3-pyridin-4-yl-pyrazolo[1,5-a]pyrimidine), a cell-permeable AMPK inhibitor (Handa et al., 2011) completely diminished the TNFα-induced generation of NO suggesting a critical role of AMPK in the regulation of eNOS activity. The latter conclusion however should be viewed with caution as Compound C has been found to exhibit some side effects, calling into question its absolute specificity towards AMPK (Kim et al., 2011; Lee et al., 2016; Liu et al., 2014). Despite this caveat one may conclude that a joint action of eNOS and AMPK is necessary for the endothelial function (NO release) under TNFα-induced stress conditions. In cells derived from eNOS-null mice a chronic AMPK activation

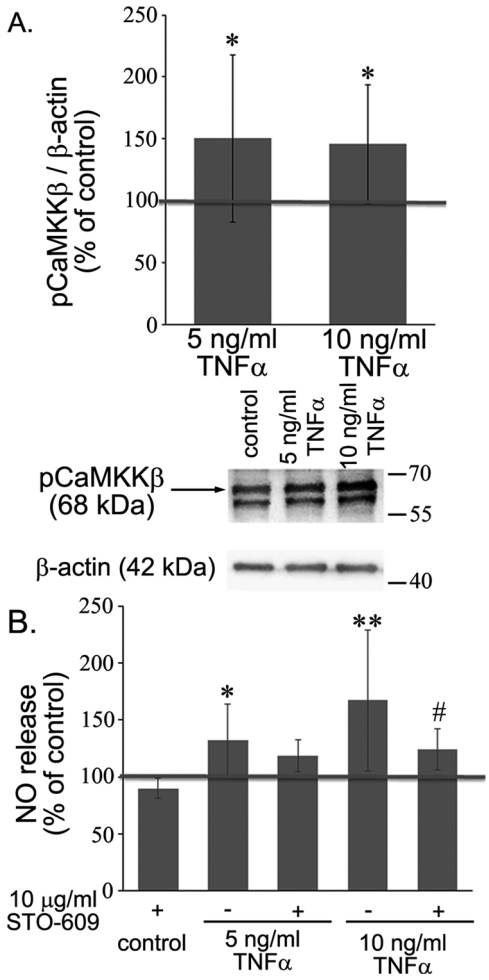

Fig. 7. Participation of CaMKKβ in TNFα-induced production of NO.
EA.hy926 cells were incubated with TNFα at 5 or 10 ng / ml for 6 h. 10 μg / ml STO-609 to inhibit CaMKKβ was added for the last 20 min of incubation.
A. Relative **p**rotein levels of pCaMKKβ are shown. Protein levels were determined by Western blotting with β-actin as a loading control. Optical density of bands was calculated densitometrically and normalized to β-actin. Representative values in control cells were taken as 100 (horizontal grey line). Mean ± SD from 12 independent experiments is shown; * $p < 0.001$ vs. control. Below representative Western blot.
B. NO content in incubation medium was determined fluorimetrically with non-cell permeable DAF. NO release by control cells (not exposed to TNFα) is taken as 100% (horizontal grey lane). Mean ± SD from 10 independent experiments for TNFα alone (the data shown here are those shown on Fig. 1) and 4 experiments with STO-609 is shown; * $p < 0.05$, ** $p < 0.001$ vs. control; # $p < 0.01$ vs. TNFα.

was insufficient to adapt them to stress. Moreover mitochondrial biogenesis during pro-survival cellular stress response was directly linked with eNOS activity by those authors (Li et al., 2016a).

AMPK is widely accepted to be the major sensor of the metabolic state not only in individual cells but also at the level of the whole organism. An increased concentration of AMP (or an increased [AMP + ADP] /[ATP] ratio) is a crucial AMPK stimulatory factor (Oakhill et al., 2011). However, the adenine nucleotide content was not affected in EA.hy926 cells exposed to TNFα, therefore the increased activity of AMPK must have been caused by factors other than energy deficit (Zhang et al., 2017). Apart from the canonical allosteric activation related to AMP binding, AMPK is also activated by phosphorylation by two major upstream kinases LKB1 and CaMKKβ; both of them were activated here. Unlike LKB1, CaMKKβ is a Ca^{2+}-dependent kinase, and both are independent of adenine nucleotides (Hawley et al.,

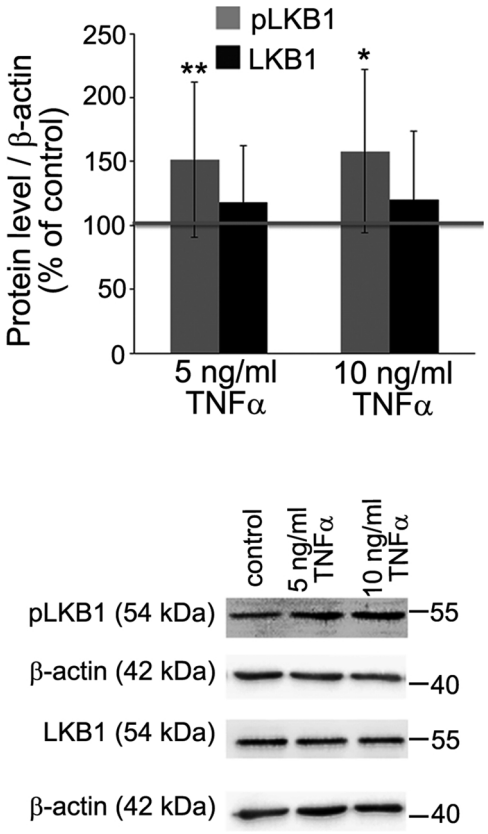

Fig. 8. Effect of TNFα on LKB1 phosphorylation.
EA.hy926 cells were incubated with TNFα at 5 or 10 ng / ml for 6 h.
Relative **p**rotein levels **of** pLKB1 and LKB1 are shown. Protein levels were determined by Western blotting with β-actin as reference. Optical density of bands was calculated densitometrically and normalized to β-actin. Representative values in control cells were taken as 100 (horizontal grey line). Mean ± SD from 14 independent experiments; * $p < 0.02$, ** $p < 0.005$ vs. control. Below representative western blot.

2005; Woods et al., 2005). It seems plausible that the slight elevation of $[Ca^{2+}]_c$ observed in TNFα-treated EA.hy926 cells had a stimulatory effect on CaMKKβ activity. The (partial) sensitivity of the TNFα-evoked phosphorylation of AMPK to STO-609 strongly confirms the participation of CaMKKβ (Tokumitsu et al., 2002). However, a possible contribution of other enzymes to the AMPK activation in TNFα-treated cells should also be considered. A similar conclusion has been drawn by Thors et al. (2011) who stimulated HUVECs with histamine or thrombin. They showed that a complete inhibition of AMPK phosphorylation was attained only if the LKB1 gene was silenced. Those observations and the only partial inhibitory effect of STO-609 on AMPK phosphorylation together with the substantially increased phosphorylation/activity of LKB1 in TNFα-treated cells led us to the conclusion that the both upstream kinases, CaMKKβ and LKB1, play a role in the AMPK activation in this experimental model. In contrast, stimulation of primary human aortic endothelial cells with estrogen resulted in AMPK activation followed by eNOS phosphorylation which both were exclusively dependent on CaMKKβ, as its inhibition with STO-609 completely abolished the estrogen-dependent phosphorylation of ACC and eNOS (Yang and Wang, 2015).

Wen et al. (2013) have suggested that the CaMKKβ/AMPK/Sirt1 pathway could be involved in the beneficial atheroprotective responses to diverse physicochemical stimuli. CaMKKβ could regulate the phosphorylation of Sirt1 which –similarly as AMPK -is also considered an energy sensor. Here TNFα substantially stimulated Sirt1 phosphorylation. Since most of the phosphorylated Sirt1 remained in the cytoplasm rather than moving to the nucleus it was capable of Sirt1 supporting the

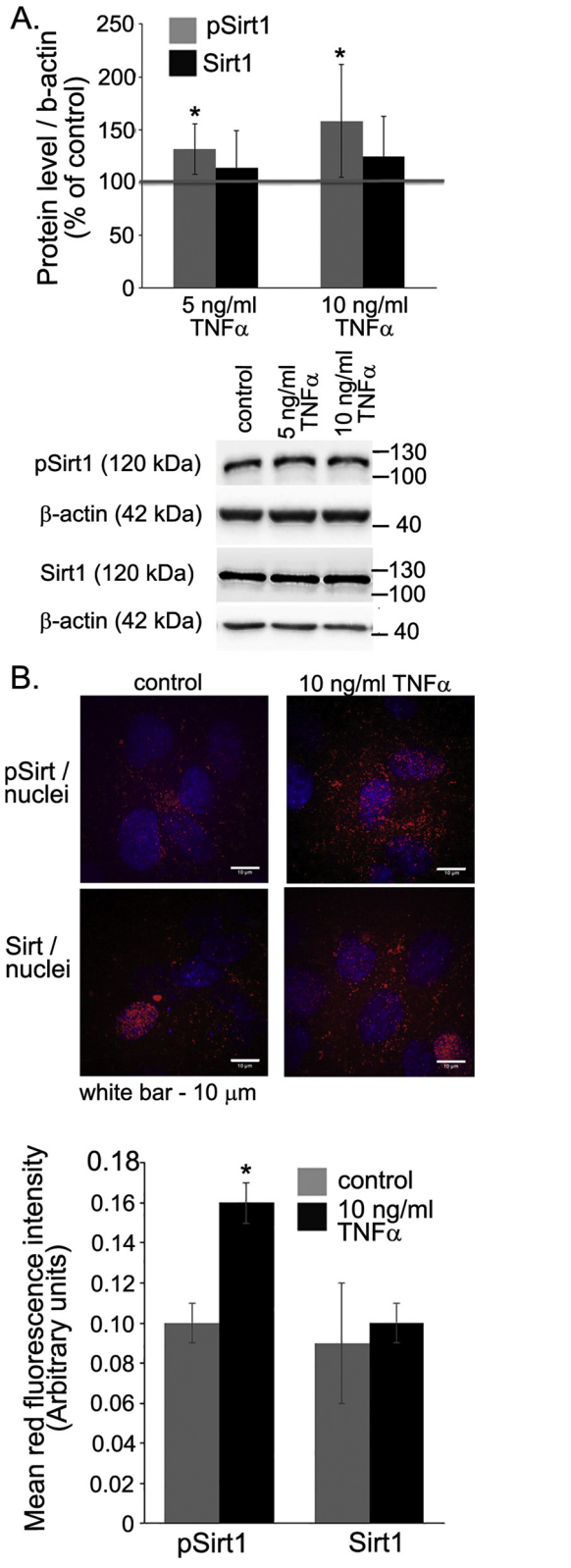

(caption on next page)

phosphorylation of eNOS, a cytoplasmic enzyme, both indirectly by stimulating AMPK activity and directly through eNOS deacetylation (Mattagajasingh et al., 2007). Our present data are in line with the previously suggested synergy of AMPK activation and elevation of Sirt1 activity leading to eNOS activation in HUVECs exposed to laminar flow (Chen et al., 2010). Furthermore, Wen et al. (2013) found an increased

Fig. 9. Effect of TNFα on Sirt1 phosphorylation and intracellular localization. EA.hy926 cells were incubated with TNFα at 5 or 10 ng / ml for 6 h.
A. Relative protein levels of pSirt1 and Sirt1 are shown. Protein levels were determined by Western blotting with β-actin as a loading control. Optical density of bands was calculated densitometrically and normalized to β-actin. Representative values in control cells were taken as 100 (horizontal grey line). Mean ± SD from 12 independent experiments is shown; * $p < 0.001$ vs. control. Below representative Western blot.
B. Fluorescence microscopy of pSirt1 and Sirt1. Red (Alexa Fluor 555) – pSirt1 or Sirt1 respectively; blue (DAPI) – nuclei. Below mean intensity of red fluorescence related to nuclear Sirt1 and pSirt1 content compared to DAPI fluorescence was quantified using CellProfiler 3.0 software. Mean ± SD from 3 independent experiments is shown; * $p < 0.004$ vs. control.

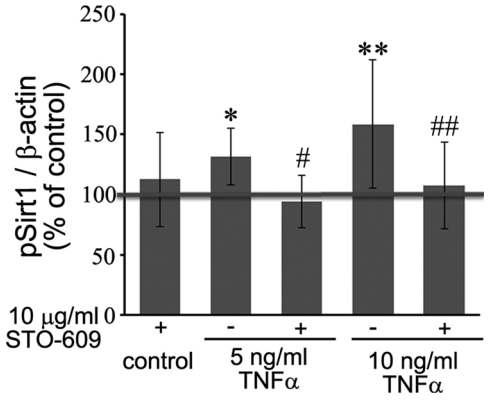

Fig. 10. Participation of CaMKKβ on TNFα-induced phosphorylation of Sirt1. EA.hy926 cells were incubated with TNFα at 5 or 10 ng / ml for 6 h. 10 μg / ml STO-609 was added for the last 20 min of incubation.
Relative protein levels of pSirt1 are shown. Protein levels were determined by Western blotting with β-actin as reference. Optical density of bands was calculated densitometrically and normalized to β-actin. Representative values in control cells were taken as 100 (horizontal grey line). Mean ± SD from 12 independent experiments for TNFα alone (the data shown here are those shown on Fig. 9A) and 6 experiment with STO-609 is shown; * $p < 0.05$, ** $p < 0.001$ vs. control; # $p < 0.05$, ## $p < 0.001$ vs. TNFα.

phosphorylation of Sirt1 in HUVECs exposed to pulsatile shear stress that was dependent on CaMKKβ activity since it was completely abolished after its silencing, similarly as we observed here after CaMKKβ inhibition by STO-609. Those authors also suggested that the phosphorylation of Sirt1 promotes its stability and elevates the deacetylase activity. Moreover, LKB1 knockdown did not affect the level of Sirt1 suggesting its downstream position to Sirt1. Apart from the deacetylation of eNOS and stimulation of NO generation (Mattagajasingh et al., 2007) Sirt1 may also deacetylate LKB1 which is associated with its movement to the cytoplasm, as has been found in HepG2 cells. Notably, these events were attributed to AMPK activation (Lan et al., 2008). Thus, the interdependence between the upstream AMPK activating kinases and Sirt1 seems to be important for proper endothelial function.

5. Conclusions

To summarize, we conclude that AMPK is essential for the eNOS activation and NO generation in EA.hy926 cells stimulated with TNFα. We also suggest a dual role of CaMKKβ as an activator of AMPK and a modulator of Sirt1 phosphorylation. In turn Sirt1 could modulate the eNOS activity directly and also indirectly through deacetylation and activation of LKB1. Thus, CaMKKβ appears to regulate eNOS activity and thereby NO formation in cells stimulated with TNFα by a mechanism linking AMPK and Sirt1. The above conclusions are presented as a cartoon in Scheme 1.

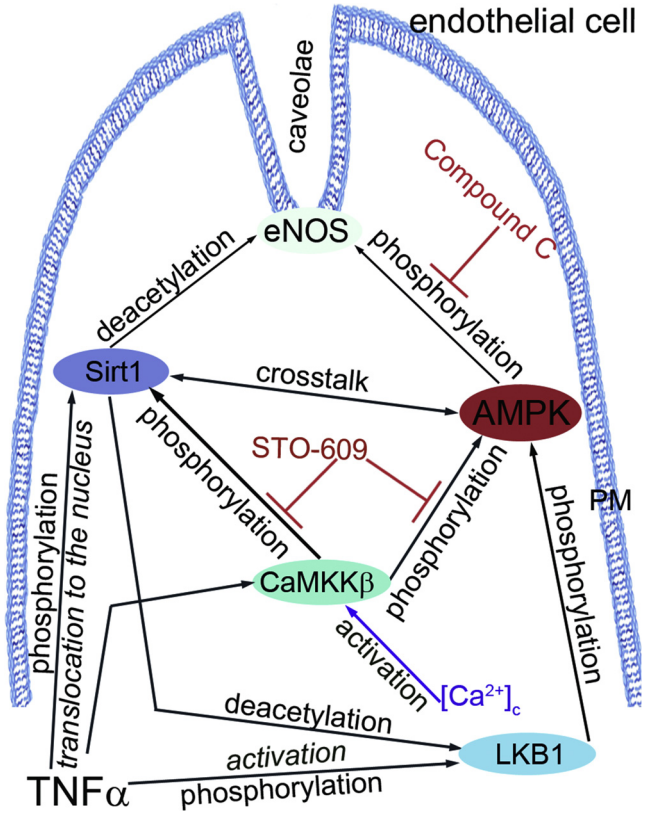

Scheme 1. Proposed mechanisms of eNOS activation by TNFα.
The crucial role of AMPK in the stimulation of eNOS activity in endothelial cells exposed to TNFα was confirmed by the inhibitory action of Compound C. AMPK activation may be catalysed by LKB1 and/or CaMKKβ. The CaMKKβ inhibitor STO-609 partially prevents the TNFα-induced increase of eNOS phosphorylation at Ser1177 and completely eliminates the Sirt1 phosphorylation. Sirt1 may influence eNOS activity directly by its deacetylation and also indirectly by modifying LKB1 activity.

Funding

This work was supported by the National Science Centre, grant number 2015/19/B/NZ3/02302.

Acknowledgements

We thank Prof. Stefan Chłopicki from JCET (Jagiellonian University, Cracow) for inspiring discussions and our colleagues Dr. Robert Jarzyna and Dr. Adam Jagielski from the Institute of Biochemistry, Faculty of Biology at the University of Warsaw for discussions and assistance in adenine nucleotide measurements.

Appendix A. Supplementary data

Supplementary material related to this article can be found, in the online version, at doi:https://doi.org/10.1016/j.biocel.2018.11.010.

References

Aggarwal, B.B., 2003. Signalling pathways of the TNF superfamily: a double-edged sword. Nat. Rev. Immunol. 3, 745–756.
Aktan, F., 2004. iNOS-mediated nitric oxide production and its regulation. Life Sci. 75, 639–653.
Bradley, E.A., Eringa, E.C., Stehouwer, C.D.A., Korstjens, I., 2010. Activation of AMP-activated protein kinase by 5-aminoimidazole-4-carboxamine-1-β-D-robofuranoside in the muscle microcirculation increases nitric oxide synthesis and microvascular perfusion. Arterioscler. Thromb. Vasc. Biol. 30, 1137–1142.
Bulotta, S., Barsacchi, R., Rotiroti, D., Borgese, N., Clementi, E., 2001. Activation of the

endothelial nitric-oxide synthase by tumor necrosis factor-α. A novel feedback mechanism regulating cell death. J. Biol. Chem. 276, 6529–6536.
Cacicedo, J.M., Gauthier, M.S., Lebrasseur, N.K., Jasuja, R., Ruderman, N.B., Ido, Y., 2011. Acute exercise activates AMPK and eNOS in the mouse aorta. Am. J. Physiol. Heart. Circ. Physiol. 301, H1255–1265.
Chen, Z., Peng, I.-C., Cui, X., Li, Y.-S., Chien, S., Shyy, J.Y.-J., 2010. Shear stress, Sirt1, and vascular homeostasis. Proc. Natl. Acad. Sci. U. S. A. 107, 10268–10273.
Chen, F., Lucas, R., Fulton, D., 2013. The subcellular compartmentalization of arginine metabolizing enzymes and their role in endothelial dysfunction. Front. Immunol. 4, 184. https://doi.org/10.3389/fimmu.2013.00184.
Childers, K.C., Garcin, E.D., 2018. Structure/function of the soluble guanylyl cyclase catalytic domain. Nitric Oxide 77, 53–64.
Choi, S., Kim, J., Kim, J.H., Lee, D.K., Park, W., Park, M., Kim, S., Hwang, J.Y., Won, M.H., Choi, Y.K., Ryoo, S., Ha, K.S., Kwon, Y.G., Kim, Y.M., 2017. Carbon monoxide prevents TNF-α-induced eNOS downregulation by inhibiting NF-κB-responsive miR-155-5p biogenesis. Exp. Mol. Med. 49, e403. https://doi.org/10.1038/emm.2017.193.
De Palma, C., Meacci, E., Perrotta, C., Bruni, P., Clementi, E., 2006. Endothelial nitric oxide synthase activation by tumor necrosis factor α through neutral sphingomyelinase 2, sphingosine kinase 1, and sphingosine 1 phosphate receptors A novel pathway relevant to the pathophysiology of endothelium. Arterioscler. Thromb. Vasc. Biol. 26, 99–105.
Devika, N.T., Jaffar Ali, B.M., 2013. Analysing calcium dependent and independent regulation of eNOS in endothelium triggered by extracellular signalling events. Mol. Biosyst. 9, 2653–2664.
Drabarek, B., Dymkowska, D., Szczepanowska, J., Zabłocki, K., 2012. TNFα affects energy metabolism and stimulates biogenesis of mitochondria in EA.hy926 endothelial cells. Int. J. Biochem. Cell Biol. 44, 1390–1397.
Dymkowska, D., Kawalec, M., Wyszomirski, T., Zabłocki, K., 2017. Mild palmitate treatment increases mitochondrial mass but does not affect EA.hy926 endothelial cells viability. Arch. Biochem. Biophys. 634, 88–95.
Escobar, D.A., Botero-Quintero, A.M., Kautza, B.C., Luciano, J., Loughran, P., Darwiche, S., Rosengart, M.R., Zuckerbraun, B.S., Gomez, H., 2015. Adenosine monophosphate-activated protein kinase activation protects against sepsis-induced organ injury and inflammation. J. Surg. Res. 194, 262–272.
Fan, R., Han, Y., Han, H., Chen, Z., Yu, B., Kou, J., Zhang, Y., 2018. DT-13 ameliorates TNF-α-induced nitric oxide production in the endothelium in vivo and in vitro. Biochem. Biophys. Res. Commun. 495, 1175–1181.
Feron, O., Belhassen, L., Kobzik, L., Smith, T.W., Kelly, R.A., Michel, T., 1996. Endothelial nitric oxide synthase targeting to caveolae. Specific interactions with caveolin isoforms in cardiac myocytes and endothelial cells. J. Biol. Chem. 271, 22810–22814.
Fleming, I., Fisslthaler, B., Dimmeler, S., Kemp, B.E., Busse, R., 2001. Phosphorylation of Thr(495) regulates Ca(2+)/calmodulin-dependent endothelial nitric oxide synthase activity. Circ. Res. 88, E68–E75.
Forstermann, U., Sessa, W.C., 2012. Nitric oxide synthases: regulation and function. Eur. Heart J. 33, 829–837.
Francis, K., Gallis, B., Corson, M.A., 2001. TNF-α inhibits flow and insulin signalling leading to NO production in aortic endothelial cell. Am. J. Physiol. Cell Physiol. 280, C1057–C1065.
García-Morales, V., Luaces-Regueira, M., Campos-Toimil, M., 2017. The cAMP effectors PKA and Epac activate endothelial NO synthase through PI3K/Akt pathway in human endothelial cells. Biochem. Pharmacol. 145, 94–101.
Godo, S., Sawada, A., Saito, H., Ikeda, S., Enkhjargal, B., Suzuki, K., Tanaka, S., Shimokawa, H., 2016. Disruption of physiological balance between nitric oxide and endothelium-dependent hyperpolarization impairs cardiovascular homeostasis in mice. Arterioscler. Thromb. Vasc. Biol. 36, 97–107.
Greif, D.M., Sacks, D.B., Michel, T., 2004. Calmodulin phosphorylation and modulation of endothelial nitric oxide synthase catalysis. PNAS 101, 1165–1170.
Handa, N., Takagi, T., Saijo, S., Kishishita, S., Takaya, D., Toyama, M., Terada, T., Shirouzu, M., Suzuki, A., Lee, S., Yamauchi, T., Okada-Iwabu, M., Iwabu, M., Kadowaki, T., Minokoshi, Y., Yokoyama, S., 2011. Structural basis for compound C inhibition of the human AMP-activated protein kinase α2 subunit kinase domain. Acta Crystallogr. D Biol. Crystallogr. 67, 480–487.
Hawley, S.A., Pan, D.A., Mustard, K.J., Ross, L., Bain, J., Edelman, A.M., Frenguelli, B.G., Hardie, D.G., 2005. Calmodulin-dependent protein kinase kinase-beta is an alternative upstream kinase for AMP-activated protein kinase. Cell Metab. 2, 9–19.
Heiss, E.H., Dirsch, V.M., 2014. Regulation of eNOS enzyme activity by posttranslational modification. Curr. Pharm. Des. 20, 3503–3513.
Hinder, F., Stubbe, H.D., Van Aken, H., Waurick, R., Booke, M., Meyer, J., 1999. Role of nitric oxide in sepsis-associated pulmonary edema. Am. J. Respir. Crit. Care Med. 159, 252–257.
Inata, Y., Kikuchi, S., Samraj, R.S., Hake, P.W., O'Connor, M., Ledford, J.R., O'Connor, J., Lahni, P., Wolfe, V., Piraino, G., Zingarelli, B., 2018. Autophagy and mitochondrial biogenesis impairment contribute to age-dependent liver injury in experimental sepsis: dysregulation of AMP-activated protein kinase pathway. FASEB J. 32, 728–741.
Kalogeris, T.J., Baines, C., Korthuis, R.J., 2014. Adenosine prevents TNFα-induced decrease in endothelial mitochondrial mass via activation of eNOS-PGC-1α regulatory axis. PLoS One 9 (6), e98459.
Kawanaka, H., Jones, M.K., Szabo, I.L., Baatar, D., Pai, R., Tsugawa, K., Sugimachi, K., Sarfeh, I.J., Tarnawski, A.S., 2002. Activation of eNOS in rat portal hypertensive gastric mucosa is mediated by TNF-alpha via the PI 3-kinase-Akt signaling pathway. Hepatology 35, 393–402.
Khaddaj Mallat, R., Mathew John, C., Kendrick, D.J., Braun, A.P., 2017. The vascular endothelium: A regulator of arterial tone and interface for the immune system. Crit. Rev. Clin. Lab. Sci. 54, 458–470.
Kim, Y.M., Kim, M.Y., Kim, H.J., Roh, G.S., Ko, G.H., Seo, H.G., Lee, J.H., Chang, K.C., 2011. Compound C independent of AMPK inhibits ICAM-1 and VCAM-1 expression in inflammatory stimulants-activated endothelial cells in vitro and in vivo. Atherosclerosis 219, 57–64.
Kofler, S., Nickel, T., Weis, M., 2005. Role of cytokines in cardiovascular diseases: a focus on endothelial responses to inflammation. Clin. Sci. (Lond.) 108, 205–213.
Kowalczyk, J.E., Beresewicz, M., Gajkowska, B., Zabłocka, B., 2009. Association of protein kinase C delta and phospholipid scramblase 3 in hippocampal mitochondria correlates with neuronal vulnerability to brain ischemia. Neurochem. Int. 55, 157–163.
Lamas, S., Michel, T., Brenner, B.M., Marsden, P.A., 1991. Nitric oxide synthesis in endothelial cells: evidence for a pathway inducible by TNF-alpha. Am. J. Physiol. 261, C634–641.
Lan, F., Cacicedo, J.M., Ruderman, N., Ido, Y., 2008. Sirt1 modulation of the acetylation status, cytosolic localisation, and activity of LKB1. Possible role in AMP-activated protein kinase activation. J. Biol. Chem. 283, 27628–27635.
Lee, Y., Park, B.H., Bae, E.J., 2016. Compound C inhibits macrophage chemotaxis through an AMPK-independent mechanism. Biochem. Biophys. Res. Commun. 469, 515–520.
Li, H., Burkhardt, C., Heinrich, U.-R., Brausch, I., Xia, N., Forstermann, U., 2003. Histamine upregulates gene expression of endothelial nitric oxide synthase in human vascular endothelial cells. Circulation 107, 2348–2354.
Li, Z., Carter, J.D., Dailey, L.A., Huang, Y.C., 2004. Vanadyl sulfate inhibits NO production via threonine phosphorylation of eNOS. Environ. Health Perspect. 112, 201–206.
Li, G., Barrett, E.J., Barrett, M.O., Cao, W., Liu, Z., 2007. Tumor necrosis factor-alpha induces insulin resistance in endothelial cells via a p38 mitogen-activated protein kinase-dependent pathway. Endocrinology 148, 3356–3363.
Li, P., Zhang, L., Zhang, M., Zhou, C., Lin, N., 2016. Uric acid enhances PKC-dependent eNOS phosphorylation and mediates cellular ER stress: a mechanism for uric acid-induced endothelial dysfunction. Int. J. Mol. Med. 37, 989–997.
Li, C., Reif, M.M., Craige, S., Kant, S., Keaney Jr, J.F., 2016a. Endothelial AMPK activation induces mitochondrial biogenesis and stress adaptation via eNOS-dependent mTORC1 signaling. Nitric Oxide 55–56, 45–53.
Liu, X., Chhipa, R.R., Nakano, I., Dasgupta, B., 2014. The AMPK inhibitor compound C is a potent AMPK-independent antiglioma agent. Mol. Cancer. Ther. 13, 596–605.
Liu, Z., Jiang, C., Zhang, J., Liu, B., Du, Q., 2016. Resveratrol inhibits inflammation and ameliorates insulin resistant endothelial dysfunction via regulation of AMP-activated protein kinase and sirtuin 1 activities. J. Diabetes 8, 324–335.
Liu, B., Xu, L., Yu, X., Li, W., Sun, X., Xiao, S., Guo, M., Wang, H., 2018. Protective effect of KLF15 on vascular endothelial dysfunction induced by TNF-α. Mol. Med. Rep. 18, 1987–1994.
Mattagajasingh, I., Kim, C.S., Naqvi, A., Yamamori, T., Hoffman, T.A., Jung, S.B., DeRicco, J., Kasuno, K., Irani, K., 2007. SIRT1 promotes endothelium-dependent vascular relaxation by activating endothelial nitric oxide synthase. Proc. Natl. Acad. Sci. U. S. A. 104, 14855–14860.
Mount, P.F., Lane, N., Venkatesan, S., Steinberg, G.R., Fraser, S.A., Kemp, B.E., Power, D.A., 2008. Bradykinin stimulates endothelial cell fatty acid oxidation by CaMKK-dependent activation of AMPK. Atherosclerosis 200, 28–36.
Murthy, S., Koval, O.M., Ramiro Diaz, J.M., Kumar, S., Nuno, D., Scott, J.A., Allamargot, C., Zhu, L.J., Broadhurst, K., Santhana, V., Kutschke, W.J., Irani, K., Lamping, K.G., Grumbach, I.M., 2017. Endothelial CaMKII as a regulator of eNOS activity and NO-mediated vasoreactivity. PLoS One 12 (10), e0186311.
Neumann, P., Gertzberg, N., Johnson, A., 2004. TNF-α induces a decrease in eNOS promoter activity. Am. J. Physiol. Lung Cell. Mol. Physiol. 286, L452–L459.
Oakhill, J.S., Steel, R., Chen, Z.P., Scott, J.W., Ling, N., Tam, S., Kemp, B.E., 2011. AMPK is a direct adenylate charge-regulated protein kinase. Science 332, 1433–1435.
Poderoso, J.J., Carreras, M.C., Lisdero, C., Riobó, N., Schöpfer, F., Boveris, A., 1996. Nitric oxide inhibits electron transfer and increases superoxide radical production in rat heart mitochondria and submitochondrial particles. Arch. Biochem. Biophys. 328, 85–92.
Rafikov, R., Fonseca, F.V., Kumar, S., Pardo, D., Darragh, C., Elms, S., Fulton, D., Black, S.M., 2011. eNOS activation and NO function: structural motifs responsible for the posttranslational control of endothelial nitric oxide synthase activity. J. Endocrinol. 210, 271–284.
Seifi, B., Kadkhodaee, M., Ranjbaran, M., Bakhshi, E., 2018. Nephroprotection through the Akt/eNOS pathway by centrally administered erythropoietin in a rat model of fixed-volume hemorrhage. Life Sci. 193, 180–185.
Subelzu, N., Bartesaghi, S., de Bem, A., Radi, R., et al., 2015. Oxidative inactivation of nitric oxide and peroxynitrite formation in the vasculature. Chapter 4 In: In: Hepel (Ed.), Oxidative Stress: Diagnostics, Prevention, and Therapy, vol. 2.
Szczygiel, A.M., Brzezinka, G., Targosz-Korecka, M., Chlopicki, S., Szymonski, M., 2012. Elasticity changes anti-correlate with NO production for human endothelial cells stimulated with TNF-α. Pflugers Arch. 463, 487–496.
Tanano, I., Nagaoka, T., Omae, T., Ishibazawa, A., Kamiya, T., Ono, S., Yoshida, A., 2013. Dilation of porcine retinal arterioles to cilostazol: roles of eNOS phosphorylation via cAMP/protein kinase A and AMP-activated protein kinase and potassium channels. Invest. Ophthalmol. Vis. Sci. 54, 1443–1449.
Thors, B., Halldórsson, H., Thorgeirsson, G., 2011. eNOS activation mediated by AMPK after stimulation of endothelial cells with histamine or thrombin is dependent on LKB1. Biochim. Biophys. Acta 1813, 322–331.
Tokumitsu, H., Inuzuka, H., Ishikawa, Y., Ikeda, M., Saji, I., Kobayashi, R., 2002. STO-609, a specific inhibitor of the Ca2+/Calmodulin-dependent protein kinase kinase. J. Biol. Chem. 277, 15813–15818.
Vanhoutte, P.M., 2018. Nitric oxide: from good to bad. Ann. Vasc. Dis. 11, 41–51.
Watts, V.L., Motley, E.D., 2009. Role of protease-activated receptor-1 in endothelial nitric oxide synthase-Thr495 phosphorylation. Exp. Biol. Med. (Maywood) 234, 132–139.
Wen, L., Chen, Z., Zhang, F., Cui, X., Sun, W., Geary, G.G., Wang, Y., Johnson, D.A., Zhu,

Y., Chien, S., Shyy, J.Y.-J., 2013. Ca^{2+}/calmodulin-dependent protein kinase kinase β phosphorylation of sirtuin 1 in endothelium is atheroprotective. Proc. Natl. Acad. Sci. U. S. A. 110, E2420–E2427.

Woods, A., Dickerson, K., Heath, R., Hong, S.P., Momcilovic, M., Johnstone, S.R., Carlson, M., Carling, D., 2005. Ca2+/calmodulin-dependent protein kinase kinase-beta acts upstream of AMP-activated protein kinase in mammalian cells. Cell. Metab. 2, 21–33.

Yang, S., Wang, J., 2015. Estrogen activates AMP-activated protein kinase in human endothelial cells via ERβ/Ca(2+)/Calmodulin-dependent protein kinase kinase β pathway. Cell. Biochem. Biophys. 72, 701–707.

Zhang, Y., Lee, T.-S., Kolb, E.M., Sun, K., Lu, X., Sladek, F.M., Kassab, G.S., Garland Jr, T., Shyy, J.Y.-J., 2006. AMP-activated protein kinase is involved in endothelial NO synthase activation in response to shear stress. Arterioscler. Thromb. Vasc. Biol. 26, 1281–1287.

Zhang, C.S., Hawley, S.A., Zong, Y., Li, M., Wang, Z., Gray, A., Ma, T., Cui, J., Feng, J.W., Zhu, M., Wu, Y.Q., Li, T.Y., Ye, Z., Lin, S.Y., Yin, H., Piao, H.L., Hardie, D.G., Lin, S.C., 2017. Fructose-1,6-bisphosphate and aldolase mediate glucose sensing by AMPK. Nature 548, 112–116. https://doi.org/10.1038/nature23275.

Żyżyńska- Granica, B., Koziak, K., 2012. Identification of suitable reference genes for real-time PCR analysis of statin-treated human umbilical vein endothelial cells. PLoS One 7 (12), e51547.